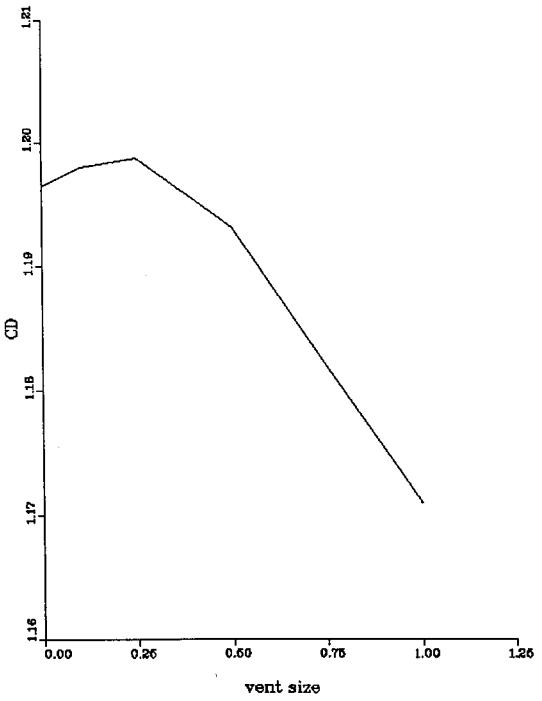

Fig. 2 C_D vs vent size, $Re = 10^6$.

on this factor. The steep dependence of the drag on the Mach number M_0 beyond $M_0 = 0.15$ is an indication of the compression wave that is being created and is consistent with experimental evidence obtained in other geometries. The small drop in the value of the drag near $M_0 = 0.4$ might be the result of numerical instabilities due to the mesh size.

C. Effect of Vent Size

Using the OVERFLOW code we simulated NSE for the geometry described in Sec. III with different vent sizes. As expected, the drag did increase as the vent size decreased. The dependence of the drag on the radius of the vent size is shown in Fig. 2. In this figure we normalized the vent size by the one used in Sec. III.

From this figure we see that for small vent sizes the drag increases considerably. This is explained by the strong vortex that is being created at the vent in this geometry.

V. Conclusions

In this research we simulated for the most part (except for the vortex algorithm) the time-independent NSE and were able to obtain time-averaged values for the drag. The results show that turbulence effects increase parachute drag by 12–15%, while canopy compliance reduces it by 7–8%. Furthermore, there is a sharp increase in the drag coefficient above Mach 0.2. We also observe that both Baldwin-Barth and the k-ε models capture correctly the effect of turbulence on the drag coefficient. The results obtained are in agreement with the experimental value when the compliant nature of the body used in the experiment is taken into account. However, based on physical arguments and results obtained using the vortex method we are led to believe that dynamical time-dependent effects can make crucial contributions to our understanding of parachute performance and design.

Acknowledgments

The author is deeply indebted to E. C. Steeves and other members of the U.S. Army RD&E Center in Natick, Massachusetts, for many discussions related to this Note. Part of this research was conducted at the center mentioned above.

References

[1]Dennis, D. R., "Recent Advances in Parachute Technology," *Aeronautical Journal*, Nov. 1983, pp. 333–342.

[2]Cockrell, D. J., "The Aerodynamics of Parachutes," AGARDOGRAPH 295, 1987.

[3]Steeves, E. C., "Analysis of Decelerators in Motion Using Computational Fluid Dynamics," *Proceedings of the AIAA 10th Aerodynamics Decelerator System Technology Conference* (Cocoa Beach, FL), 1989, pp. 269–278 (AIAA Paper 89-0931).

[4]Stein, K., private communication, U.S. Army Natick Research, Development, and Engineering Center, Natick, MA, 1991.

[5]Humi, M., "Drag Computation by Vortex Methods," *Journal of Aircraft*, Vol. 29, No. 5, 1992, pp. 819–822.

[6]Tennekes, H., and Lumley, J. L., "A First Course in Turbulence," Massachusetts Inst. of Technology Press, Cambridge, MA, 1972.

[7]Markatos, N. C., "The Mathematical Modelling of Turbulent Flows," *Applied Mathematical Modeling*, Vol. 10, No. 6, 1986, pp. 190–220.

[8]Buning, P. B., Chan, W. M., Renzi, K. J., Sondak, D. L., Chiu, I. T., and Slotnick, J. P., "OVERFLOW Users Manual," NASA Ames Research Center, Version 1.6w, Moffett Field, CA, Oct. 1992.

[9]Gorski, J. J., and Haussling, H. J., *DTNS Users Manual*, David Taylor Naval Ship RD&E Center, Bethesda, MD, 1993.

[10]Humi, M., "Three Dimensional Vortex Method for Parachutes," *International Journal for Numerical Methods in Fluids*, Vol. 16, No. 10, 1993, pp. 879–890.

[11]Benjamin, T. B., "Fluid Flow with Flexible Boundaries," *Proceedings of the 11th International Congress in Applied Mathematics* (Munich, Germany), 1964, pp. 109–126.

Estimation of Supersonic Leading-Edge Thrust by a Euler Flow Model

C. de Nicola,* R. Tognaccini,† and P. Visingardi‡
University of Naples, 80125 Naples, Italy
and
L. Paparone§
Centro Italiano Ricerche Aerospaziali, 81043 Capua, Italy

Nomenclature

AR	=	aspect ratio
C_A	=	axial force coefficient
C_D	=	drag coefficient
C_L	=	lift coefficient
$C_{L\,\mathrm{des}}$	=	design lift coefficient
C_N	=	normal force coefficient
M_∞	=	freestream Mach number
S_s	=	suction parameter
α	=	incidence
ΔC_D	=	drag coefficient due to lift

Presented as Paper 94-1821 at the AIAA 12th Applied Aerodynamics Conference, Colorado Springs, CO, June 20–23, 1994; received July 28, 1994; revision received Oct. 19, 1994; accepted for publication Oct. 19, 1994.

*Associate Professor, Dipartimento di Progettazione Aeronautica, P.le Tecchio 80. Associate Member AIAA.

†Staff Research Scientist, Dipartimento di Progettazione Aeronautica, P.le Tecchio 80. Member AIAA.

‡Contract Research Scientist, P.le Tecchio 80.

§Staff Research Scientist, via Maiorise. Member AIAA.

Introduction

THIS Note deals with the applicability of the Euler equations based flow solvers to the aerodynamic design and analysis of supersonic transport aircraft configurations at cruise conditions. Considerable improvements are expected due to the capability of the Euler flow model to predict, in principle, nonlinear effects as an alternative to the analysis traditionally carried out by using linear methods.

This research area has been clearly addressed by Carlson[1] and Mann.[2] They indicated as a key problem establishing if the strongly nonlinear phenomenon of the leading-edge thrust can be taken into account in the design of supersonic wings. Furthermore, Carlson pointed out the question of whether or not the Euler flow model is able to predict thrust, even for the case of sharp leading-edge wing, since the Euler results he presented did not capture any level of suction at all angles of attack. Present results, obtained by using a multiblock structured Euler flow simulation system,[3] show the capability of the Euler flow model to predict the leading-edge thrust for sharped wings with a good level of accuracy.

Flow Simulation

The numerical scheme used in the current simulation system is based on the well-known central space discretization with self-adaptative explicit second- and fourth-order artificial dissipation proposed by Jameson. Since the added explicit viscosity is nonlinear, this scheme can be considered as intermediate between the classical methods and the modern shock-capturing methods, in which the numerical dissipation is strongly nonlinear. Although it was mainly developed for transonic flow calculations, a number of supersonic applications can be found in literature.[4]

Large dispersive oscillations are the typical problems related to the application of central schemes to supersonic flow simulation, in particular when discontinuities oblique with respect to the curvilinear coordinates of the grid are present. The main problem is associated to the simplified upwinding procedure introduced by the second-order artificial viscosity. Nevertheless, appropriate wall boundary conditions have shown a large influence on the accuracy of the results. Boundary conditions based on the solution of a half-Riemann problem at the wall have provided solutions clearly more accurate than that obtained by classical pressure extrapolations.[5]

Results

The geometry used for the three-dimensional tests is a swept arrow wing, being available a detailed experimental data set.[6] The main peculiarities of the Carlson wing are sharp leading edge, 70-deg leading-edge sweep, absence of curvature ($C_{L\text{des}} = 0$).

A C-C type grid topology consisting of four blocks has been used. The grid is made up of 332,800 cells on the finest level, with 2560 cells on the wing.

The diagrams of the aerodynamic coefficients evaluated by the Euler simulation are presented in Figs. 1–3. The forces have been computed by integration of the surface pressure distribution. Friction drag effects, evaluated on the basis of flat plate assumption, have been added to allow comparisons with the experiments. Furthermore, the Euler results are compared with the forces obtained by using the method of Carlson, based on the solution of the linearized theory integral equations and semiempirical nonlinear corrections. The agreement on the normal force coefficient vs incidence is excellent, it is interesting to note the behavior of the axial force coefficient that is invariant with the angle of attack for a flat wing in the linearized theory. As suggested by Carlson[1] "Any departure from this behaviour is interpreted as an attainment of some amount of leading edge thrust."

Artificial dissipation enables Euler calculations to avoid singularities at leading edges and makes accurate simulation of the primary vortex separation at sharp leading edges possible, at least for moderate angles of attack (Fig. 4).

In spite of the slight overestimation of the axial force coefficient at the highest incidences, the comparison with the experiment is quite satisfactory and is indicative of the capture of a certain level of thrust by the Euler flow.

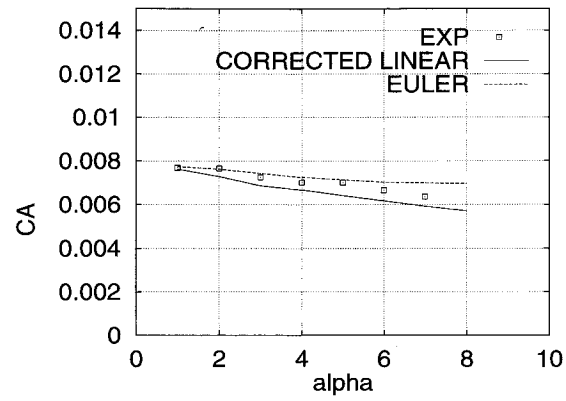

Fig. 1 Carlson arrow wing, $M_\infty = 2.05$, axial force coefficient vs incidence.

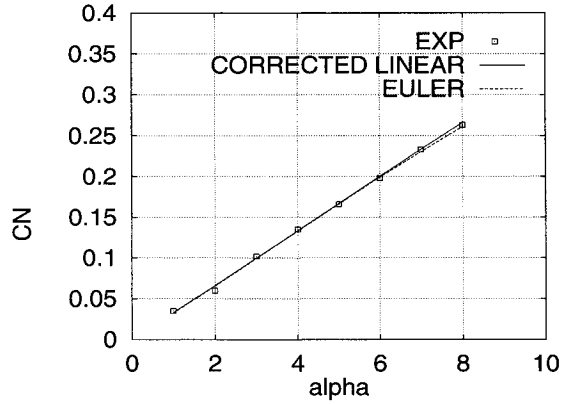

Fig. 2 Carlson arrow wing, $M_\infty = 2.05$, normal coefficient vs incidence.

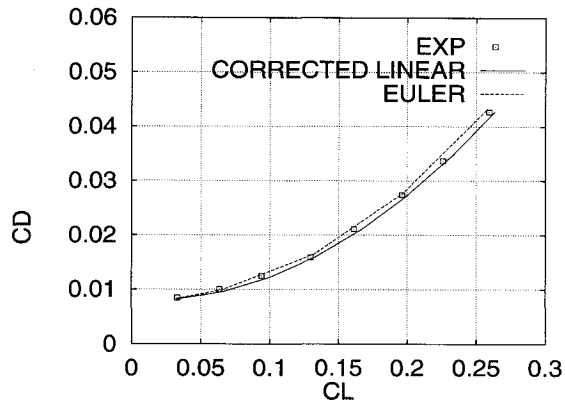

Fig. 3 Carlson arrow wing, $M_\infty = 2.05$, drag vs lift coefficient.

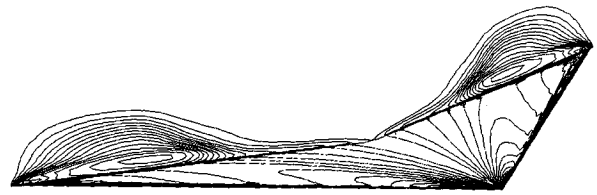

Fig. 4 Carlson arrow wing, $M_\infty = 2.05$, $\alpha = 8$ deg, total pressure loss isolines.

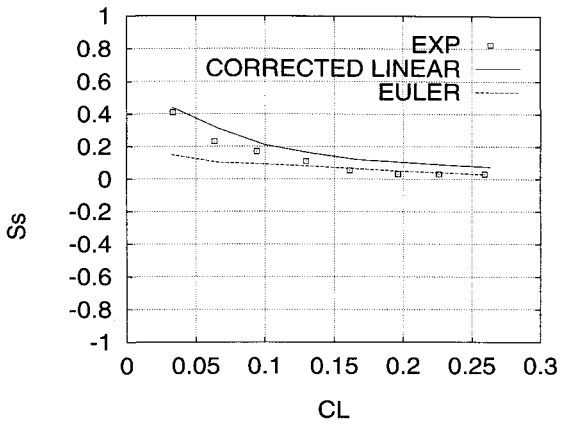

Fig. 5 Carlson arrow wing, $M_\infty = 2.05$, suction parameter vs lift coefficient.

A better understanding of the results can be obtained by introducing the suction parameter:

$$S_s = \frac{C_L \cdot \tan(C_L/C_{L\alpha}) - \Delta C_D}{C_L \cdot \tan(C_L/C_{L\alpha}) - C_L^2/(\pi \cdot AR)}$$

With such parameter the computed drag is compared with the upper bound (i.e., drag of a flat wing with no thrust and vortex forces) and the lower bound obtained in case of a wing with an elliptical span load distribution and the full amount of theoretical leading-edge thrust. These two limit cases are obtained for $S_s = 0$ and $S_s = 1$, respectively. Figure 5 shows that the Euler solution provides a reasonable level of suction for the highest incidences. Although the values of S_s are wrong at low incidences, the discrepancies in terms of the axial coefficient are still low. This fact can be explained by noting that when lift tends to zero, also the difference between the upper and lower bound is vanishing. These results are in disagreement with the Euler computation presented by Carlson[1] for the same wing configuration and obtained by a space-marching method. Present results seem to explain this difference by the poor accuracy at the leading edge of the pressure distribution in the Carlson[1] solution.

Conclusions

The main results of the present study can be summarized as follows:

1) Central space discretized schemes can provide reasonable flow solutions and included the primary vortex effects; the numerical model can influence the solution accuracy (for supersonic flow in particular it is strongly affected by wall boundary conditions).

2) Force coefficients obtained by pressure integration are in good agreement with the experiments.

3) The behavior of the axial force vs incidence reveals the capability of the Euler flow model to predict leading-edge thrust.

4) Euler simulation can effectively support the supersonic wing design since nonlinear semiempirical correction depends on the availability of large experimental database and is limited to specified families of wing planform.

References

[1]Carlson, H. W., and Mann, M. J., "Survey and Analysis of Research on Supersonic Drag-Due-to-Lift Minimization with Recommendations for Wing Design," NASA TP 3202, Sept. 1992.

[2]Mann, M. J., and Carlson, H. W., "Aerodynamic Design of Supersonic Cruise Wings with a Calibrated Linearized Theory," *Journal of Aircraft*, Vol. 31, No. 1, 1994, pp. 35–41.

[3]Amendola, A., Tognaccini, R., Boerstoel, J. W., and Kassies, A., *Validation of a Multi-Block Euler Flow Solver with Propeller-Slipstream Flows*, Vol. 2, AGARD-CP-437, May 1988, pp. 1–15.

[4]Moitra, A., "Euler Solutions for High-Speed Flow About Complex Three-Dimensional Configurations," AIAA Paper 86-0246, Jan. 1986.

[5]De Nicola, C., Tognaccini, R., Visingardi, P., and Paparone, L., "Progress in the Aerodynamic Analysis of Inviscid Supersonic Flow Fields Around Complex Aircraft Configurations," *Proceedings of the AIAA 12th Applied Aerodynamics Conference* (Colorado Springs, CO), Vol. 1, AIAA, Washington, DC, 1994, pp. 128–136 (AIAA Paper 94-1821).

[6]Carlson, H. W., "Pressure Distributions at Mach Number 2.05 on a Series of Highly Swept Arrow Wings Employing Various Degrees of Twist and Camber," NASA TN D-1264, May 1962.

Computation of Vortex Breakdown on a Rolling Delta Wing

Raymond E. Gordnier*
U.S. Air Force Wright Laboratory,
Wright–Patterson Air Force Base, Ohio 45433-7913

Introduction

REFERENCE 1 presents a detailed description of the computation of several different "roll-and-hold" maneuvers (see Table 1) for an 80-deg sweep delta wing at 30-deg angle of attack. This Note focuses on one interesting feature observed for case III, dynamically induced vortex breakdown of the upward-moving edge vortex during a portion of the roll maneuver. Dynamic motion has clearly been shown to influence vortex breakdown over delta wings. Experimental investigations of delta-wing rock by both Arena[2] and Ng et al.[3] show large hysteresis loops in vortex breakdown location due to time lags in the motion of the breakdown position. Ericsson and Hanff[4] report that the dynamic effect of vortex breakdown in experiments by Hanff[5] on a 65-deg sweep rolling delta wing is controlled to a large extent by roll-rate induced camber. Pitching motions also exhibit a lag of the vortex breakdown[6] as compared to the static situation. Gursul et al.[7] have also shown in experiments with an unsteady freestream that breakdown can occur on a delta wing with increasing unsteady effects, even if no breakdown is observed in a steady freestream, similar to the situation arising in this Note.

Discussion

For the rolling motion of case III the right vortex (upward motion) exhibits a small region of vortex breakdown near the trailing edge during a portion of the roll maneuver. Figure 1 tracks the location of the vortex burst point (defined as the location of the forward stagnation point) from the initial appearance of burst at a roll angle $\phi \approx 7.77$ deg, to when the vortex burst disappears, $\phi \approx -30.95$ deg. The vortex burst crosses the wing trailing edge at a roll angle, $\phi = 3.22$ deg. The maximum upstream penetration of the breakdown is $X/L = 0.914$ at $\phi = -17.28$ deg. The burst point also shows a spanwise motion across the wing due to the rolling motion.

Presented as Paper 93-2975 at the AIAA 24th Fluid Dynamics Conference, Orlando, FL, July 6–9, 1993; received Feb. 1, 1994; revision received Feb. 19, 1995; accepted for publication Feb. 20, 1995.

*Aerospace Engineer, CFD Research Branch, Aeromechanics Division. Senior Member AIAA.